Mössbauer Studies of Ferrous Sulfate†

Hang Nam Ok
Department of Physics, Yonsei University, Seoul, Korea
(Received 29 June 1971)

We have considered in detail the effects of the low symmetry of the Fe^{2+} ion site in $FeSO_4$ on the electronic energy-level splittings and electric field gradient. Using x-ray crystallographic data and a high-speed computer, direct lattice-sum calculations have been carried out, yielding the electronic energy splittings and their corresponding eigenfunctions. Temperature dependence of quadrupole splittings calculated using these eigenfunctions is in good agreement with the experimental values taken up to 600 °K. The direction of the maximum electric field gradient at low temperatures is calculated to be nearly parallel to the crystallographic b_0 axis, which is consistent with neutron-diffraction and Mössbauer measurements. The ground orbital state is a singlet separated by $7|\lambda|$ from the first excited state, and the calculated quadrupole splitting and asymmetry factor are 3.38 mm/sec and 0.48, respectively, in agreement within experimental errors with the experimental values at low temperature.

I. INTRODUCTION

$FeSO_4$ is an orthorhombic crystal and the tetramolecular unit cell has the lattice constants[1] $a_0 = 5.255$ Å, $b_0 = 7.975$ Å, $c_0 = 6.590$ Å. Each Fe^{2+} ion is surrounded by six oxygen atoms occupying the vertices of a much-distorted octahedron, as shown in Figs. 1 and 2. The symmetry of each ferrous ion consists of a reflection plane and a twofold axis perpendicular and parallel to the a_0 axis, respectively. Magnetic-susceptibility and neutron-diffraction measurements[2] have established that the magnetic moments agree with those expected from the ferrous ions with completely quenched orbital angular momentum, and the spin orientation is parallel to the b_0 axis to an accuracy of 2° below the Néel temperature of 21 °K. Mössbauer measurements[3] show that the principal axis of the maximum electric-field-gradient tensor is parallel to the b_0 axis, the sign of e^2qQ is positive, and the asymmetry parameter is 0.4 at liquid-helium temperature. Using the crystal-field theory, Ingalls interpreted Mössbauer data[4] taken at four different temperatures between liquid-nitrogen temperature and room temperature. He took into account axial and rhombic fields in addition to the cubic field. However, as shown in Figs. 1 and 2, the distortion of the octahedron is too great to be approximated only by cubic, axial, and rhombic fields. The purpose of this paper is to present Mössbauer data taken over a wider temperature range up to 600 °K, and to interpret the quadrupole splittings in terms of direct lattice-sum calculation using x-ray crystallographic data and a high-speed computer.

II. SAMPLE PREPARATION AND MÖSSBAUER SPECTROMETRY

The anhydrous sulfate of iron was prepared by heating the hydrated salt at 300 °C for 3 h in high vacuum. The conversion of the hydrated salt to anhydrous sulfate was observed to take place at 500 °K by Mössbauer measurements. Only the orthorhombic crystal structure of the anhydrous

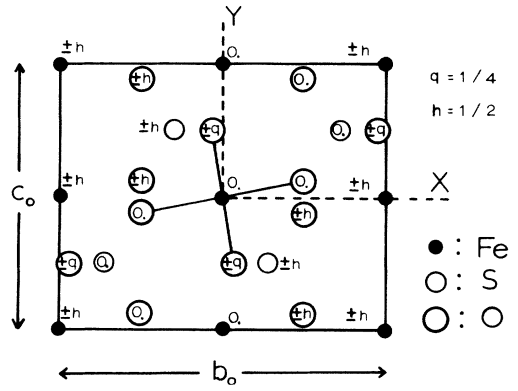

FIG. 1. $FeSO_4$ structure projected onto the b_0c_0 plane. Ion positions are given in fractional units of a_0.

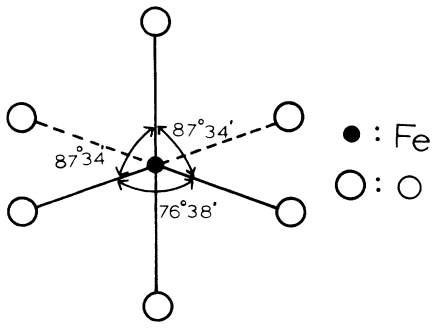

FIG. 2. Distorted octahedral coordination of the ferrous ion in $FeSO_4$.

sulfate sample was detected in x-ray diffraction patterns. Specimens for both Mössbauer and x-ray measurements were handled in a sealed Plexiglass glove box with a high-purity nitrogen-gas atmosphere.

A Mössbauer spectrometer with an electromechanical drive system was used and has already been described elsewhere.[5] The source was Co^{57} in palladium, purchased from the New England Nuclear Corporation. The temperature measurements in the Mössbauer oven and cryostat were made by means of copper-constantan and iron-constantan thermocouples. All the Mössbauer results presented here have been obtained by a least-squares fitting of two Lorentzians to Mössbauer spectra with the help of the CDC 3300 computer of the Korea Institute of Science and Technology.

III. THEORY

The electric field gradient at Fe^{2+} in a crystal consists of two terms, namely, the direct lattice contribution and the contribution from the valence electron of the Fe^{2+} ion. The lattice contribution can be calculated by evaluating the following lattice sum:

$$(V_{ij})_{\text{lat}} = \sum_k \frac{q_k(3R_{ik}R_{jk} - \delta_{ij}R_k^2)}{R_k^5} \quad (i,j = x,y,z) , \tag{1}$$

where q_k and (R_{xk}, R_{yk}, R_{zk}) are the charge and the coordinates of the kth ion. For the contribution of the valence electron one must consider electronic level splittings due to crystal-field and spin-orbit coupling, and each level's contribution to the electric field gradient at the Fe^{57} nucleus.

The crystal-field energy acting on a $3d$ electron of Fe^{2+} in $FeSO_4$ may be expanded in terms of spherical harmonics,[6]

$$V = \sum_{l,m} r^l A_l^m Y_l^{m*}(\theta,\phi) ,$$

where

$$A_l^m = -\frac{4\pi}{2l+1} \sum_i \frac{q_i e^2}{R_i^{l+1}} Y_l^{m*}(\theta_i,\phi_i) . \tag{2}$$

$\vec{r}(r,\theta,\phi)$ is the position vector of the unpaired $3d$ electron of Fe^{2+}, and q_i and $\vec{R}_i(R_i,\theta_i,\phi_i)$ are the charge and position vectors of the ith ion, respectively. When we take x, y, and z axes along the b_0, c_0, and a_0 directions of a $FeSO_4$ crystal, respectively (Fig. 1), the xy plane becomes a reflection plane. Using the same argument as for Fe^{2+} ion at the Ca(II) site in apatite,[6] V can be written as

$$V = r^2[A_2^0 Y_2^0 + 2\,\text{Re}\,(A_2^2 Y_2^2)] + r^4[A_4^0 Y_4^0 + 2\,\text{Re}(A_4^2 Y_4^2 + A_4^4 Y_4^4)] , \tag{3}$$

where Re represents the real part of the quantities in parentheses. Including the spin-orbit coupling, we have a 25×25 perturbation matrix between the five orbital states Y_2^m $(m = 0, \pm 1, \pm 2)$ and the five spin states of the ground term ^5D of the Fe^{2+} ion. Diagonalization of this matrix will give electronic energy levels E_n and their eigenfunctions $\Phi_n (n = 1, 2, \ldots, 25)$. The total electric-field-gradient tensor can be written as

$$\langle V_{ij}\rangle = (1-R)\langle (V_{ij})_{\text{val}}\rangle + (1-\gamma_\infty)(V_{ij})_{\text{lat}} \quad (i,j = x,y,z) , \tag{4}$$

where $\langle (V_{ij})_{\text{val}}\rangle$ is the statistical average of the electric-field-gradient tensor of the valence electron taken over the above 25 states Φ_n at temperature T. The Sternheimer factors, $(1-R)$ and $(1-\gamma_\infty)$, represent the effects of polarization of the ferriclike $(^6S, 3d^5)$ core by the electric field gradients of the valence and lattice charge distributions. This nine-component tensor must be diagonalized to give the principal values $\langle V_{x'x'}\rangle$, $\langle V_{y'y'}\rangle$, and $\langle V_{z'z'}\rangle$. The quadrupole splitting becomes

$$(eQ/2)\langle V_{z'z'}\rangle(1+\tfrac{1}{3}\eta^2)^{1/2} , \tag{5}$$

where Q is the nuclear quadrupole moment of the 14.4-keV state in Fe^{57}, and η is the asymmetry parameter of the electric field gradient. x', y', z' axes are chosen in such a way that $|\langle V_{z'z'}\rangle| > |\langle V_{y'y'}\rangle| > |\langle V_{x'x'}\rangle|$.

IV. RESULTS AND DISCUSSION

The Mössbauer spectra of Fe^{57} in $FeSO_4$ were taken at temperatures ranging from 78 to 600 °K. The temperature dependence of the quadrupole splittings is shown in Fig. 3. It is noteworthy that the quadrupole splittings are large and decrease slowly with increasing temperature. Large values

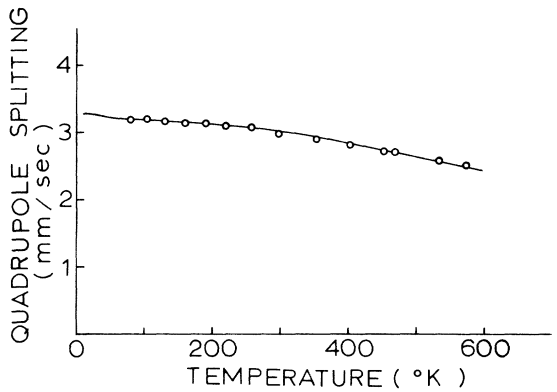

FIG. 3. Temperature dependence of the quadrupole splittings of Fe^{57} in $FeSO_4$; solid line indicates theoretical values.

TABLE I. Calculated values[a] of A_l^m.

l	m	A_l^m/e^2
2	0	$-0.0025(3)\ (4\pi/5)^{1/2}$
2	2	$[0.0383(2)-0.0084(1)i](4\pi/5)^{1/2}$
4	0	$-0.0135(1)\ (4\pi/9)^{1/2}$
4	2	$[-0.0350(1)+0.0108(0)i]\ (4\pi/9)^{1/2}$
4	4	$[0.0158(1)-0.0163(0)i]\ (4\pi/9)^{1/2}$

[a]Lengths are calculated in Å. Errors in last place are given in parentheses.

of quadrupole splittings and the slow variation with increasing temperature suggest that the crystal field is much larger than the spin-orbit coupling. In applying the crystal-field theory we performed the direct lattice summations on a CDC 3300 computer by using a point-charge model. The calculations were made by evaluating the nine-component electric-field-gradient tensor $(V_{ij})_{\rm lat}$ in Eq. (1) and five of the A_l^m in Eq. (2). The summations were carried out over all the ions that are contained within a chosen radial distance from the central ferrous ion. The sphere of radius 28 Å chosen for $FeSO_4$ was sufficient for convergence. The charge of the ferrous ion was taken to be +2, and the charges of the oxygen and sulfur ions in $SO_4^=$ were derived from Pauling's estimates.[7] The possible polarization of oxygen was neglected. The results are shown in Tables I and II. In this calculation $Q=0.20$ b and $(1-\gamma_\infty)=12$ were used.[8] The orbital states of the ground term ^5D of the free ferrous ion are split into five levels by the crystal field V of Eq. (3), as shown in Fig. 4. The energy splittings and the eigenfunctions are calculated by diagonalizing a 5×5 interaction matrix of $\langle Y_2^m|V|Y_2^{m'}\rangle$ $(m,m'=0,\pm1,\pm2)$, and are shown in Table III. In this calculation, $\langle r^2\rangle=1.39$ a.u. and $\langle r^4\rangle=4.51$ a.u. were used, following Freeman and Watson.[9] The ground orbital state is a singlet well separated from the first excited level by $(7.0\pm0.1)|\lambda|$, where the spin-orbit coupling constant λ is that for the free ion[10]: $\lambda=-103\ \mathrm{cm}^{-1}$. The existence of a well-separated singlet is in

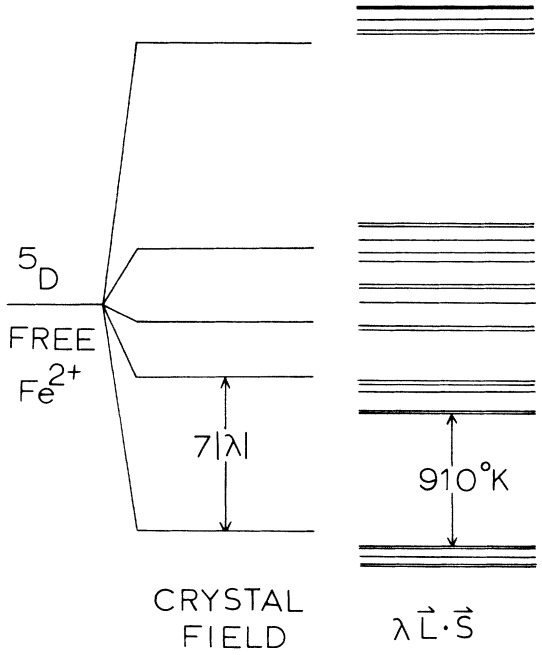

FIG. 4. Energy-level schemes of Fe^{2+} in $FeSO_4$.

agreement with the neutron-diffraction measurements.[2] Using the ground-state orbital wave function we calculated the quadrupole splitting and asymmetry factor of (3.4 ± 0.1) mm/sec and 0.48 ± 0.01, respectively. These are within experimental error in agreement with the values[3] (3.6 ± 0.2) mm/sec and 0.4 ± 0.1 obtained at liquid-helium temperature. In this calculation the best values[8,9] $\langle r^{-3}\rangle=4.8$ a.u., $(1-R)=0.68$, and $Q=0.20$ b were used. To get the temperature dependence of the quadrupole splitting we took into account the spin-orbit coupling $\lambda\vec{L}\cdot\vec{S}$, and diagonalized the 25×25 matrix of $V+\lambda\vec{L}\cdot\vec{S}$ among 25 states consisting of five orbital states and five spin states of the ^5D term. The resulting energy splittings are shown in Fig. 4, and the temperature dependence of the quadrupole splittings is shown by the solid line in Fig. 3. It can be seen that the theoretical curve fits very well the experimental

TABLE II. Calculated values[a] of the direct-lattice contribution to the quadrupole splittings.

ij	$\frac{1}{2}eQ(1-\gamma_\infty)\ (V_{ij})_{\rm lat}$ (mm/sec)
xx	−0.3466(5)
xy	−0.0737(1)
xz	0
yy	0.329(2)
yz	0
zz	0.018(2)

[a]Errors in last place are given in parentheses.

TABLE III. Crystal-field splittings and their corresponding eigenfunctions.[a]

Energy splittings in units of $\lvert\lambda\rvert$	Eigenfunctions
11.96(2)	$[-0.550(1)+0.097(2)i]Y_2^2+[0.608(2)+0.086(2)i]Y_2^0$ $+[-0.501(1)-0.246(3)i]Y_2^{-2}$
2.55(4)	$0.707(0)Y_2^1+[0.707(0)+0.010(3)i]Y_2^{-1}$
−0.81(1)	$0.707(0)Y_2^1+[0.707(0)-0.006(2)i]Y_2^{-1}$
−3.36(3)	$[-0.684(8)+0.160(8)i]Y_2^2-0.111(3)iY_2^0$ $+[0.684(8)+0.159(8)i]Y_2^{-2}$
−10.33(3)	$[0.272(8)+0.347(5)i]Y_2^2+[0.427(8)-0.655(8)i]Y_2^0$ $+[0.207(8)+0.389(5)i]Y_2^{-2}$

[a]Errors in last place are given in parentheses.

values of the quadrupole splittings over the wide range of temperature up to 600 °K. In our calculation of energy splittings and quadrupole splittings we have neglected covalency effects.[8] The direction cosines of the principal axes, x', y', and z' of the electric-field-gradient tensor at 4 °K are calculated to be x' axis (0, 0, 1), y' axis (-0.03682 ± 0.00007, 0.99932 ± 0.00001, 0), and z' axis (0.99932 ± 0.00001, 0.03682 ± 0.00007, 0). This means that the direction of the maximum electric field gradient is nearly parallel to the b_0 axis within $(2.12 \pm 0.01)°$, which is consistent with neutron-diffraction measurements[2] and Mössbauer measurements[3] at liquid-helium temperature.

†Work supported by the Ministry of Science and Technology, Republic of Korea.

[1]R. W. G. Wyckoff, *Crystal Structures* (Wiley-Interscience, New York, 1964), Vol. III.
[2]B. C. Frazer and P. J. Brown, Phys. Rev. 125, 1283 (1962).
[3]K. Ono and A. Ito, J. Phys. Soc. Japan 19, 899 (1964).
[4]R. Ingalls, Phys. Rev. 133, A787 (1964).
[5]Hang Nam Ok, Kyun Nahm, and Soo Wan Lee, New Phys. (Korea) 10, 117 (1970).
[6]Hang Nam Ok, Phys. Rev. 185, 477 (1969).
[7]L. Pauling, *The Nature of the Chemical Bond* (Cornell U. P., Ithaca, New York, 1960), p. 321.
[8]A. J. Nozik and M. Kaplan, Phys. Rev. 159, 273 (1967).
[9]A. J. Freeman and R. E. Watson, Phys. Rev. 131, 2566 (1963).
[10]R. E. Trees, Phys. Rev. 82, 683 (1951).

PHYSICAL REVIEW B VOLUME 4, NUMBER 11 1 DECEMBER 1971

Ultrasonic Attenuation and Mn^{55} Nuclear Acoustic Resonance in MnTe

K. Walther
Philips Forschungslaboratorium Hamburg GmbH, Hamburg 54, *Germany*
(Received 24 February 1970; revised manuscript received 17 May 1971)

The ultrasonic attenuation in MnTe for longitudinal waves with propagation vector in the hexagonal plane was measured as a function of temperature for frequencies up to 530 MHz. The attenuation below the Néel temperature comprises both background losses and an extraordinarily intense (attenuation up to 300 dB/cm) temperature-dependent resonance absorption caused by Mn^{55} nuclear acoustic resonance. Extrapolation to zero temperature yields a resonance frequency $f_{NAR} = 466.5$ MHz and a hyperfine field $H_n = 442$ kOe. Theoretical expressions for the sound absorption due to electronic and nuclear spins were derived. Comparison with the measured magnetic-field dependence of background and nuclear-acoustic-resonance (NAR) absorption suggests that spins located in domains rather than inside domain walls are mainly responsible for the observed effects. The spin-flop fields, observed in the NAR experiments, are much higher than the values calculated from anisotropy constants and susceptibilities. Good agreement between experiments and theory is obtained for $H \gg H_{SF}$.

I. INTRODUCTION

Nuclear-magnetic-resonance studies in antiferromagnetic materials provide detailed information about the magnetic ordering, since nuclei in these substances experience a strong hyperfine field H_n proportional to the electronic sublattice magnetization M. The corresponding nuclear resonances occur in the frequency range of several hundred MHz and can be excited both with rf magnetic fields (NMR)[1] and ultrasonic waves [nuclear acoustic resonance (NAR)].[2-4]

An extraordinarily intense ultrasonic resonance absorption in the antiferromagnetic semiconductor MnTe was observed by the author[3] and interpreted as being due to NAR of the Mn^{55} nucleus. Strength and magnetic-field dependence of the resonance were explained previously[3] in terms of the driving field enhancement mechanism occurring within domain walls.[5] In this paper we present a more detailed account on the Mn^{55} NAR in MnTe, demonstrating that spins located in domains are mainly responsible for the observed effects, contrary to the previous interpretation.[3]

The antiferromagnetic modification of MnTe crystallizes in the NiAs structure,[6] in which the magnetic cations form a simple hexagonal lattice. The Néel temperature, below which antiferromagnetic ordering occurs, is $T_N = 306.7$ °K.[3,7-9] In the antiferromagnetic phase the average spin directions in each plane perpendicular to the hexagonal axis (c plane) are parallel to each other and antiparallel to those of the Mn atoms in the adjacent c plane.[10-12] A strong anisotropy force causes the spin directions to be oriented perpendicular to the c axis. MnTe is thus an "easy-plane" antiferromagnet with